Journal of Innovative Optical Health Sciences
Vol. 7, No. 3 (2014) 1450029 (9 pages)

DOI: 10.1142/S1793545814500291

World Scientific
www.worldscientific.com

Coagulation and ablation of biological soft tissue by quantum cascade laser with peak wavelength of 5.7 μm

Keisuke Hashimura*, Katsunori Ishii*, Naota Akikusa†, Tadataka Edamura†, Harumasa Yoshida† and Kunio Awazu*,‡,§,¶

*Medical Beam Physics Laboratory, Division of Sustainable Energy and Environmental Engineering, Graduate School of Engineering
Osaka University, Japan

†Hamamatsu Photonics, K. K., Japan

‡Graduate School of Frontier Biosciences, Osaka University, Japan

§The Center for Advanced Medical Engineering and Informatics
Osaka University, Japan

¶awazu@see.eng.osaka-u.ac.jp

Received 24 October 2013
Accepted 15 January 2014
Published 17 March 2014

Molecules such as water, proteins and lipids that are contained in biological tissue absorb mid-infrared (MIR) light, which allows such light to be used in laser surgical treatment. Esters, amides and water exhibit strong absorption bands in the 5–7 μm wavelength range, but at present there are no lasers in clinical use that can emit in this range. Therefore, the present study focused on the quantum cascade laser (QCL), which is a new type of semiconductor laser that can emit at MIR wavelengths and has recently achieved high output power. A high-power QCL with a peak wavelength of 5.7 μm was evaluated for use as a laser scalpel for ablating biological soft tissue. The interaction of the laser beam with chicken breast tissue was compared to a conventional CO_2 laser, based on surface and cross-sectional images. The QCL was found to have sufficient power to ablate soft tissue, and its coagulation, carbonization and ablation effects were similar to those for the CO_2 laser. The QCL also induced comparable photothermal effects because it acted as a pseudo-continuous wave laser due to its low peak power. A QCL can therefore be used as an effective laser scalpel, and also offers the possibility of less invasive treatment by targeting specific absorption bands in the MIR region.

Keywords: Quantum cascade laser; mid-infrared wavelength; CO_2 laser; biological soft tissue; laser–tissue interaction.

1. Introduction

1.1. *Development of quantum cascade lasers*

Quantum cascade lasers (QCLs) are a new type of semiconductor laser that utilize sub-band transitions in semiconductor multilayer structures. Typical semiconductor lasers are based on a p-n junction, and photons are generated by recombination of electrons and holes. The emission wavelength of such lasers is determined by the bandgap of the semiconductors used in the active region and has an upper limit of about 2.5 μm. On the other hand, light emission from a QCL occurs by transitions between sub-bands formed in an artificially designed semiconductor multilayer structure (quantum cascade). It is possible to tune the emission wavelength over a wide range because it is determined primarily by the thickness of the individual layers.[1] In 1994, Faist *et al.* succeeded in fabricating a QCL with a peak emission wavelength of 4.3 μm based on intersub-band transitions in an InGaAs/InAlAs multiple quantum well and superlattice structure.[2] In 2001, continuous wave (CW) room-temperature emission at mid-infrared (MIR) wavelengths was reported,[3] followed by terahertz emission in 2002.[4] Thus, QCLs are capable of emission at both mid- and far-infrared wavelengths.

The MIR region is important because many molecules exhibit strong characteristic absorption bands at these wavelengths, associated with stretching and bending vibration modes. Studies have been carried out on the use of QCLs for detecting trace amounts of atmospheric gases and also for breath analysis.[5–7] Recently, considerable progress has been made with regard to increasing the output power of QCLs. In 2011, Bai *et al.* achieved an average power of 5.1 W in CW mode for a QCL with a peak emission wavelength of 4.9 μm operating at room temperature.[8]

1.2. *MIR lasers in laser surgery*

Biological tissue contains molecules such as water, proteins and lipids, which absorb MIR light due to excitation of vibration and rotation modes of their molecular bonds, and this can be used for laser surgical treatment. Conventional lasers currently in clinical use include Ho:YAG (wavelength: 2.1 μm), Er,Cr:YSGG (2.79 μm), Er:YAG (2.94 μm) and CO_2 (10.6 μm) lasers.[9–12] However, there are strong absorption bands in the 5–7 μm wavelength range associated with esters ($\sim$ 5.75 μm), amides ($\sim$ 6 μm) and water ($\sim$ 6 μm) that cannot be taken advantage of using such lasers.[13] It is therefore considered likely that improved cutting efficiency and biological tissue removal would be possible using a laser that can emit at such wavelengths.

As discussed above, there are no laser devices in current clinical use that can emit at wavelengths of 5–7 μm. Although CO lasers are capable of emission wavelengths of 4.7–8.2 μm,[14] they are rarely used in clinical practice because of the toxicity of CO. Free electron lasers (FELs) can also emit MIR regions and many studies have been conducted.[15–19] However, FELs are too large to be practical for clinical applications. Other alternatives are wavelength conversion using nonlinear optical techniques such as difference-frequency generation (DFG)[20] or optical parametric oscillator (OPO),[21] and as Raman-shifted lasers.[22,23] There are some reports of pre-clinical studies using these lasers.

1.3. *Objective of this study*

The present study focused on the QCL, since it is a compact semiconductor-based laser, it has recently become capable of high output power, and it can easily be made to emit in the desired wavelength range of 5–7 μm. If it can be confirmed that the output power is sufficient, it is considered to have considerable potential as a laser treatment device for cutting and coagulating biological tissue.

The objective of this study was therefore to evaluate a high-power QCL with a peak emission wavelength of 5.7 μm for use as a laser scalpel for ablating biological soft tissue. The effect of the laser beam on chicken breast tissue was investigated and compared with that of a conventional medical CO_2 laser, because CO_2 laser is most commonly used as a laser scalpel in many hospital departments.

2. Materials and Methods

2.1. *Samples*

The chicken breast tissue used for the laser irradiation tests was cut into pieces 2–3 cm in size. Its absorption coefficient (μ_a) at the peak emission

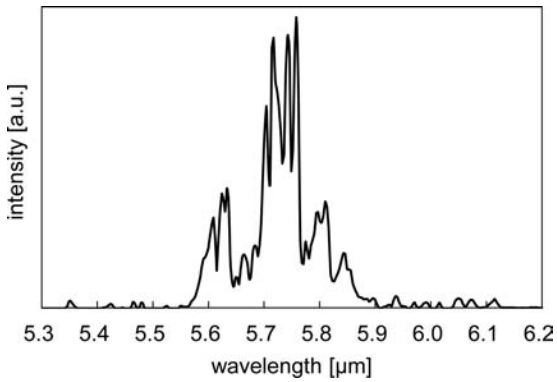

Fig. 1. Output spectrum of QCL.

wavelength of the two lasers was first determined using pieces with sizes of approximately 1 cm that were sliced to a thickness of about 10 μm using a freezing microtome (CM1850, Leica Microsystems Co. Ltd., Germany). The sliced sections were placed on BaF_2 substrates and their thicknesses were measured using a confocal laser scanning microscope (LEXT OLS3100, Olympus, Japan). The absorbance spectrum was measured using a Fourier-transform infrared spectrometer (MB3000, ABB, Switzerland) coupled with an infrared microscope (μMax, Pike Technologies, USA). From the measured thickness d and absorbance A, μ_a was calculated using Eq. (1).

$$\mu_a = \frac{A}{d \log \mathrm{e}} = \frac{A}{0.434d}. \quad (1)$$

The density ρ of the chicken breast was determined to be 1.06 g/cm^3, based on the measured volume and mass. This was used for estimating temperature rise of the samples in Sec. 4.1.

2.2. *Light sources and irradiation method*

The QCL (prototype) was manufactured by Hamamatsu Photonics, K.K., Japan and has a peak emission wavelength of 5.7 μm. It produces a pulsed output when a square wave current is injected. The pulse width and the repetition rate can be varied between 20–500 ns and 1–1000 kHz, respectively. In this study, they were respectively set to 500 ns and 1000 kHz (duty ratio: 50%) for stable operation at maximum output power. The injection current to the laser element was 1.0 A. Figure 1 shows the measured output spectrum of the laser in air, which extends over a wavelength range of about 5.6–5.9 μm, with the maximum intensity occurring at a wavelength of 5.76 μm.

Figure 2(a) shows the optical setup used for QCL irradiation. The height of XYZ stage was adjusted so that the focus of the parabolic mirror was on the surface of the samples. Using the knife-edge method, the beam size was determined to be 180 × 280 μm^2 (full width at half maximum). The average power density was set to 1250 or 2500 W/cm^2 (the energy per pulse: 0.495 or 0.990 μJ/pulse, single pulse fluence: 1.25 or 2.50 mJ/cm^2/pulse) and the irradiation time was 1, 2 or 5 s. A motorized stage (SGSP20-20(XY), SIGMA KOKI, Japan) was used for cross-sectional observations, and it moved linearly at a constant rate. The scanning speed was 280, 140 or 56 μm/s, and was calculated by dividing the

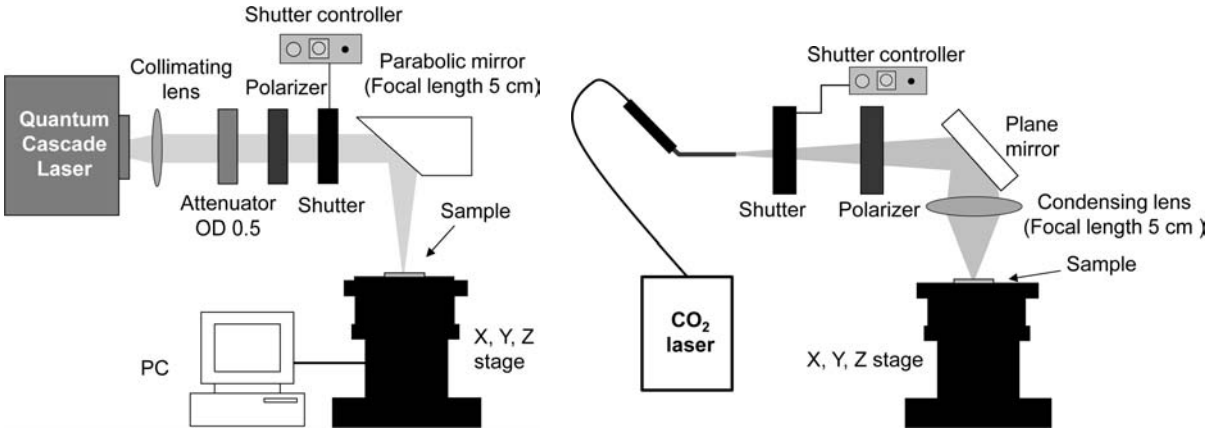

Fig. 2. Optical setup used for QCL and CO_2 laser irradiation.

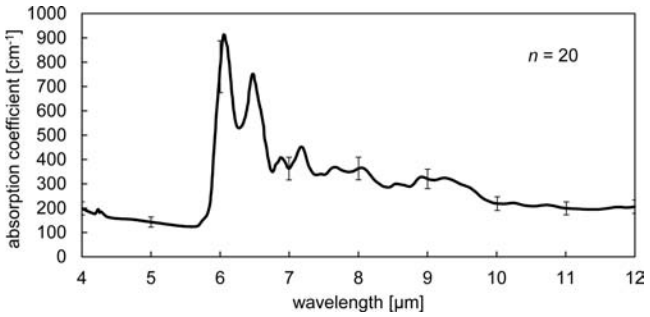

Fig. 3. Absorption coefficient for chicken breast tissue.

beam size (280 μm) by the irradiation time per spot (1, 2 or 5 s).

The CO_2 laser was a medical/dental CO_2 device (Lezawin CH S, J. Morita Mfg. Corp., Japan) with a peak emission wavelength of 10.6 μm. Figure 2(b) shows the optical setup used for CO_2 laser irradiation. The beam size was $300 \times 260\,\mu m^2$, and the same power densities and irradiation times were used as in the case of the QCL. The scanning speed of the motorized stage was 260, 130 or 52 μm/s.

2.3. *Observations*

After laser irradiation, the surface of the samples was imaged using a digital camera (PowerShot G9, Canon, Japan). For cross-sectional observations, the samples were frozen, sliced to a thickness of about 10 μm using the freezing microtome, and stained with hematoxylin and eosin (HE staining). Cross-sectional images were then obtained using an optical microscope (BIOREVO BZ-9000, Keyence, Japan). The coagulation width and ablation depth were measured from the surface and cross-sectional images.

3. Results

3.1. *Absorption coefficient for chicken breast tissue*

The measured thickness of the chicken breast tissue was $11.0 \pm 1.4\,\mu m$ ($n = 20$). Figure 3 shows μ_a as a function of wavelength, obtained from the absorbance spectrum. At the peak emission wavelengths of 5.76 and 10.6 μm for the QCL and the CO_2 laser, μ_a was 150 and 210 cm^{-1}, respectively.

3.2. *Irradiation effects produced by QCL*

Figure 4 shows surface and cross-sectional images of the chicken breast tissue following QCL irradiation. From Fig. 4(a), it can be seen that coagulation, carbonization and ablation occurred for all irradiation conditions. The area affected was larger than the beam size and increased with irradiation time. The cross-sectional images of the stained samples shown in Fig. 4(b) indicate that the ablation depth also increased with irradiation time. Figure 5 shows the dependence of the coagulation width and the ablation depth on the irradiation time. At 2500 W/cm^2, the ablation depth was larger

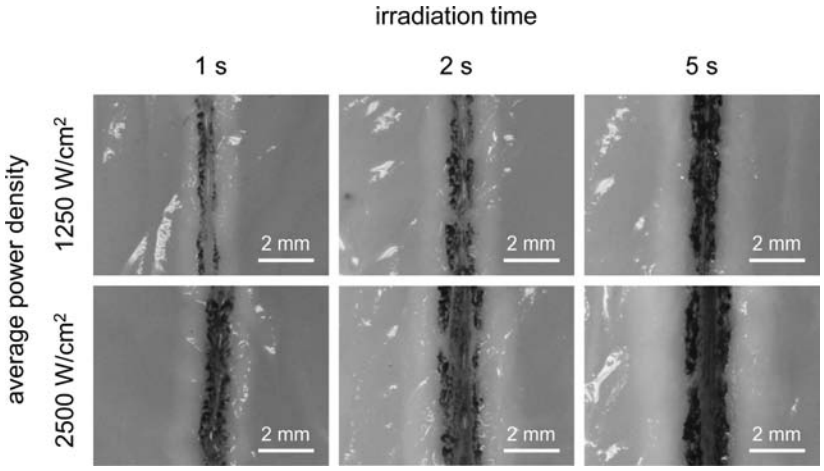

(a)

Fig. 4. Effects of QCL irradiation on chicken breast tissue. (a) Surface view and (b) cross-sectional view.

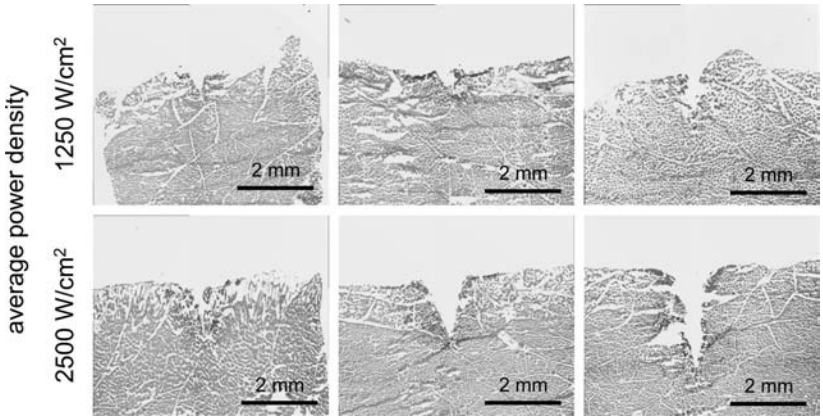

(b)

Fig. 4. (*Continued*)

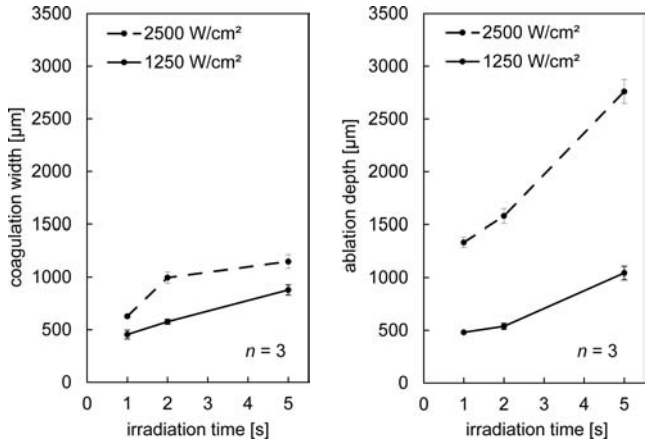

(a) (b)

Fig. 5. Relationship between QCL irradiation time and (a) coagulation width (b) ablation depth.

than the coagulation width, and increased more strongly with irradiation time.

3.3. *Irradiation effects produced by CO_2 laser*

Figure 6 shows surface and cross-sectional images of the samples irradiated by the CO_2 laser. As with QCL irradiation, coagulation, carbonization and ablation occurred. However, a larger amount of carbonization was induced by CO_2 laser irradiation. From the cross-sectional images in Fig. 6(b), the ablation depth was also larger for the CO_2 laser. Figure 7 shows the dependence of the coagulation width and the ablation depth on the CO_2 laser irradiation time. For both 1250 and 2500 W/cm^2, the ablation depths were larger for the CO_2 laser than

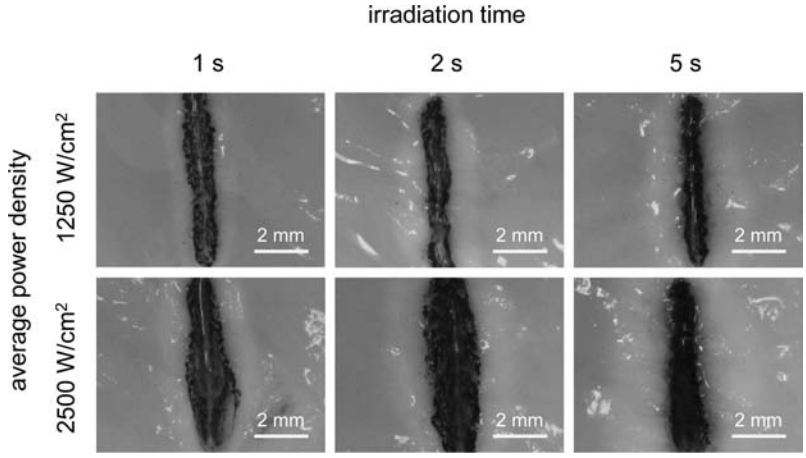

(a)

Fig. 6. Effects of CO_2 laser irradiation on chicken breast tissue. (a) Surface view and (b) cross-sectional view.

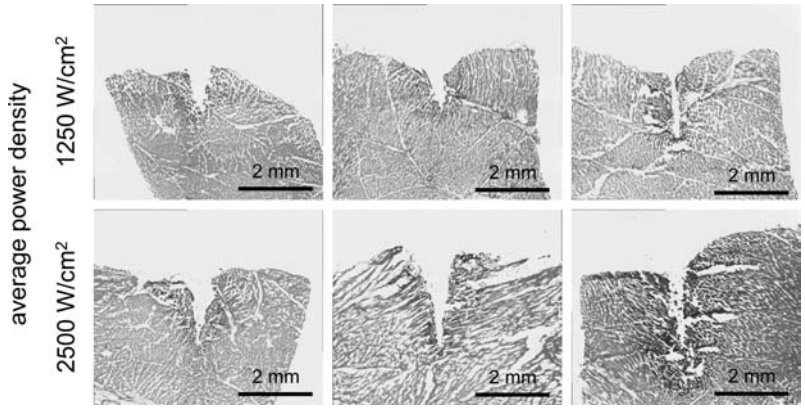

(b)

Fig. 6. (*Continued*)

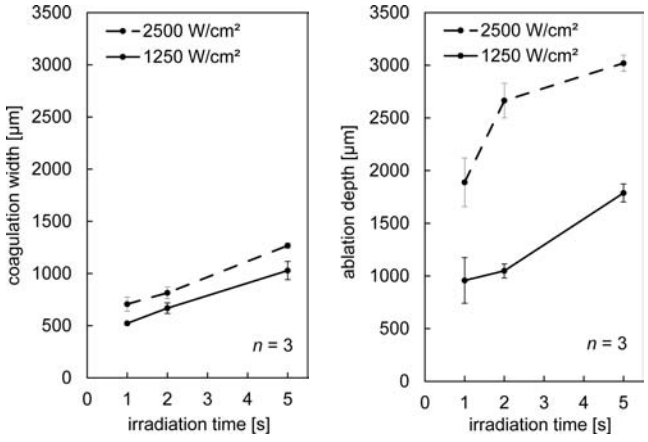

(a) (b)

Fig. 7. Relationship between CO_2 laser irradiation time and (a) coagulation width and (b) ablation depth.

for the QCL. However, similar coagulation widths were observed for both lasers.

4. Discussion

4.1. *Interaction between chicken breast tissue and laser beam*

The interaction between the samples and the laser beams is now considered based on the absorption properties of chicken breast tissue. The μ_a shown in Fig. 3 was determined under dry conditions. The samples used for the irradiation tests had a water content of about 70%, which is typical for chicken breast tissue. To compensate for this, 0.3 times the μ_a value for dry tissue was added to 0.7 times the μ_a value for water to give the equivalent μ_a value for wet tissue. Figure 8 shows μ_a for wet tissue, dry tissue and water. The presence of water is seen to have a strong influence. At a wavelength of 5.76 and 10.6 μm, the μ_a value for wet tissue is 350 and 520 cm^{-1}, respectively, which indicates that the CO_2 laser beam is more strongly absorbed than the QCL beam. It should be noted that the samples become dry as the irradiation time increases, so that μ_a becomes close to the value for dry tissue. Coagulation and carbonization are also considered to affect the μ_a value.

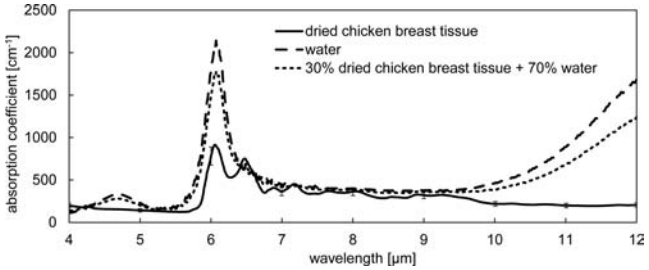

Fig. 8. Absorption coefficient for dry chicken breast tissue, water and 30% dried chicken breast tissue + 70% water.

The light penetration depth $\delta_p (= 1/\mu_a)$ for dry tissue is calculated to be 66 and 48 μm at a wavelength of 5.76 and 10.6 μm, respectively. For wet tissue, these values are 29 and 19 μm. The thermal relaxation time τ_{therm} is given by

$$\tau_{\text{therm}} = \frac{\delta^2}{4\alpha} = \frac{1}{4\alpha\mu_a^2}, \tag{2}$$

where α is the thermal diffusivity, which depends on the water content in the samples. For soft tissue

with a water content of 0% and 70%, α has been reported to be 1.02×10^{-3} and $1.42 \times 10^{-3}\,\mathrm{cm}^2/\mathrm{s}$, respectively.[24] Therefore, τ_{therm} for dry chicken breast tissue is calculated to be 11 and 5.6 ms at a wavelength of 5.76 and 10.6 μm, respectively. For wet tissue, these values are 1.4 and 0.65 ms. Because the CO_2 laser operates in CW mode, the interaction time τ_{int} between the laser beam and the sample is equivalent to the irradiation time. Since $\tau_{\mathrm{int}} \gg \tau_{\mathrm{therm}}$, CO_2 laser irradiation induces photothermal effects in the samples. On the other hand, since the QCL operates in pulsed mode, it might be thought that no such photothermal effects would be produced. However, a single pulse is insufficient to cause ablation and thus tissue removal relies on the accumulation of heat from multiple pulses. The QCL thus acts as a quasi-CW laser, and photothermal effects are induced in the samples. The temperature increase associated with such photothermal effects gives rise to reactions such as coagulation, vaporization and carbonization, which is consistent with the results for the irradiated samples in the present study.

The temperature rise ΔT in biological tissue due to absorption of laser energy is given by

$$\Delta T = \frac{(1-R)\mu_a F_0 e^{-\mu_a z}}{\rho c}, \tag{3}$$

where R is the reflectance, F is the irradiation energy density, z is the depth from the irradiated surface and c is the specific heat of the tissue.[25] For MIR wavelengths, R can be considered to be 0. The value of c depends on the water content in the samples. For a water content of 0% and 70%, it has been reported to be 1.70 and 3.45 J/g/K, respectively.[24] Figure 9 shows ΔT as a function of z for wet and dry tissue under QCL or CO_2 laser irradiation for an average power density of $1250\,\mathrm{W/cm}^2$ and an irradiation time of 0.1 ms ($F_0 = 125\,\mathrm{mJ/cm}^2$). This calculation assumes that all of the laser beam energy is used to increase the temperature. In fact, as the temperature increases, the tissue coagulates, carbonizes and vaporizes. In particular, when the temperature reaches about 374°C, which is the critical point for water,[26] the tissue is strongly ablated due to volume expansion (vaporization and the associated reaction force). In addition, we did not consider heat diffusion to surrounding tissue because the irradiation time of 0.1 ms is shorter than τ_{therm} (0.65–11 ms). For $z > 60\,\mu$m, ΔT for CO_2 laser irradiation is smaller than that for QCL irradiation. However, in the present study, it was found that the ablation depth was larger for the CO_2 laser. This is thought to be because the CO_2 laser energy is absorbed more strongly in the surface region of the sample, giving rise to significant vaporization of water and soft tissue, thus enhancing the ablation rate.

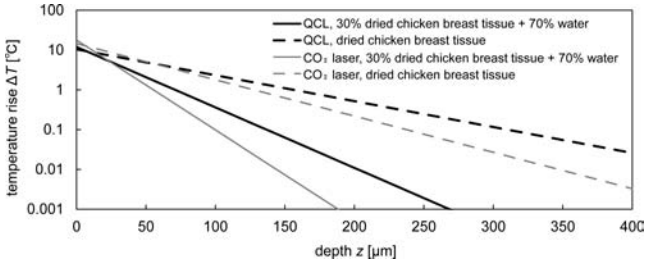

Fig. 9. Temperature rise ΔT as function of depth z in sample for $F_0 = 125\,\mathrm{mJ/cm}^2$.

4.2. *Potential of QCL for laser surgery*

As described in Secs. 3.2 and 3.3, both types of laser caused similar effects in the samples, although the ablation depth was larger for the CO_2 laser. In addition, in Sec. 4.1, it was shown that both laser beams are expected to interact with the samples in a similar way. Thus, a QCL operating at 5.7 μm can also be used as a laser scalpel. However, it is shown that the QCL induced large amounts of thermal damage as well as the CO_2 laser. In the other studies using different MIR lasers, laser ablation of soft biological tissue with much smaller thermal damage has already been achieved.[21–23] Therefore, QCL is not the best laser system in regard to thermal effects. However, QCLs are considered to be still useful because they are very compact and simple compared to other laser systems. Improving thermal effects by QCL irradiation is thus an important problem. For limiting thermal damage, higher peak power is required because if the targeted tissue can be vaporized by one pulse, the heat is removed before it diffuses into surrounding tissues.

In some situations where less invasive treatment is required, lasers operating in the 5–7 μm wavelength range may even offer some advantages. Recently, selective ablation of atherosclerosis lesions using a QCL at a wavelength of 5.7 μm has been investigated.[27] This is based on an absorption band at 5.75 μm associated with the stretching vibration mode of C=O bonds in cholesteryl esters.

Less invasive caries treatment at a wavelength of 5.8 μm has also been studied.[28] In both studies, a nanosecond pulsed laser beam produced by DFG was used. However, such a system is too large to use in actual clinical practice, so that a QCL is an attractive alternative. When less invasive treatment is required, a laser beam with a smaller wavelength spread is desirable for treatments that target specific molecules. The QCL used in the present study had a Fabry-Perot type resonator (FP-QCL), giving rise to a relatively large spread of 5.6–5.9 μm. To overcome this, a distributed feedback QCL (DFB-QCL) can be used, in which a specific wavelength is amplified because the resonator is in the form of a diffraction grating. Therefore, a narrow wavelength spectrum can be realized using a DFB-QCL, although the output power is generally lower than that for a FP-QCL. Thus, additional measures are needed such as stacking multiple laser elements and using a cooling system.

Although the QCL used in the present study was cooled with liquid nitrogen, a more convenient Peltier-cooled QCL has already been developed.[29] In addition, the same hollow-core optical fiber that is used with Er:YAG dental lasers and CO_2 medical/dental lasers can be used to deliver MIR light. Therefore, a surgical QCL device is considered to be realizable, and by optimizing the output wavelength spread, opens up the possibility of less invasive treatment.

5. Conclusion

The output power of a QCL with a peak emission wavelength of 5.7 μm was found to be sufficiently high to ablate biological soft tissue. Since it operated as a pseudo-CW laser, it produced the same photothermal effects as a conventional CO_2 surgical laser, leading to coagulation, carbonization and ablation. In addition to its use as a laser scalpel, a QCL offers the possibility of less invasive treatment by targeting specific MIR absorption bands.

Acknowledgment

This work was supported by JSPS KAKENHI Grant Number 24241209.

References

1. F. Capasso, "High-performance mid-infrared quantum cascade lasers," *Opt. Eng.* **49**, 111102 (2010).
2. J. Faist, F. Capasso, D. L. Sivco, C. Sirtori, A. L. Hutchinson, A. Y. Cho, "Quantum cascade laser," *Science* **264**, 553–556 (1994).
3. M. Beck, D. Hofstetter, T. Aellen, J. Faist, U. Östele, M. Ilegems, E. Gini, H. Melshior, "Continuous wave operation of a mid-infrared semiconductor laser at room temperature," *Science* **295**, 301 (2002).
4. R. Köhler, A. Tredicucci, F. Beltram, H. E. Beere, E. H. Linfield, A. G. Davies, D. A. Ritchie, R. C. Iotti, F. Rossi, "Terahertz semiconductor-heterostructure laser," *Nature* **417**, 156 (2002).
5. G. Hancock, G. Ritchie, J. van Helden, R. Walker, "Applications of midinfrared quantum cascade lasers to spectroscopy," *Opt. Eng.* **49**, 111121 (2010).
6. J. B. McManus, M. S. Zahniser, D. D. Nelson, Jr., J. H. Shorter, S. Herndon, E. Wood, R. Wehr, "Application of quantum cascade lasers to high-precision atmospheric trace gas measurements," *Opt. Eng.* **49**, 111124 (2010).
7. T. H. Risby, F. K. Tittel, "Current status of mid-infrared quantum and interband cascade lasers for clinical breath analysis," *Opt. Eng.* **49**, 111123 (2010).
8. Y. Bai, N. Bandyopadhyay, S. Tsao, S. Slivken, M. Razeghi, "Room temperature quantum cascade lasers with 27% wall plug efficiency," *Appl. Phys. Lett.* **98**, 181102 (2011).
9. M. J. Bader, D. Tilki, G. Gratzke, R. Sroka, C. G. Stief, O. Reich, "Ho:YAG laser: Treatment of vesicourethral structures after radical prostatectomy," *World J. Urol.* **28**, 169–172 (2010).
10. S. Kelbauskiene, N. Baseviciene, K. Goharkhay, A. Moritz, V. Machiulskeiene, "One-year clinical results of Er,Cr:YSGG laser application in addition to scaling and root planning in patients with early to moderate periodontitis," *Lasers Med. Sci.* **26**, 445–452 (2011).
11. S. Renvert, C. Lindahl, A. R. Jansåker, G. R. Persson, "Treatment of peri-implantitis using an Er:YAG laser on an air-abrasive device: A randomized trial," *J. Clin. Periodontol.* **38**, 65–73 (2011).
12. A. M. Chapas, L. Brightman, S. Sukal, E. Hale, D. Daniel, L. J. Bernstein, R. G. Geronemus, "Successful treatment of acneiform scarring with CO_2 ablative fractional resurfacing," *Lasers Surg. Med.* **40**, 381–386 (2008).
13. G. Socrates, *Infrared and Raman Characteristic Group Frequencies*, 3rd Edition, John Wiley & Sons Ltd., England (2001).
14. Yu. M. Andreev, A. A. Ionin, I. O. Kinyaevsky, Yu. M. Klimachev, A. Yu, Kozlov, A. A. Kotkov, G. V. Lanskii, A. V. Shaiduko, "Broadband carbon monoxide laser system operating in the wavelength

range of 2.5–8.3 μm," *Quantum Electron.* **43**, 139–143 (2013).
15. G. Edwards, R. Logan, M. Copeland, L. Reinisch, J. Davidson, B. Johnson, R. Maciunas, M. Mendenhall, R. Ossoff, J. Tribble, J. Werkhaven, D. O'Day, "Tissue ablation by a free-electron laser tuned to the amide II band," *Nature* **371**, 416–419 (2004).
16. J. Youn, G. M. Peavy, V. Venugopalan, "Free electron laser ablation of articular and fibro-cartilage at 2.79, 2.9, 6.1, and 6.45 μm: Mass removal studies," *Lasers Surg. Med.* **36**, 202–209 (2005).
17. M. Heya, Y. Fukami, H. Nagats, Y. Nishida, K. Awazu, "Gelatin ablation wavelength dependency in the range of 5.6–6.7 μm using a mid-infrared free electron laser," *Nucl. Instrum. Methods. Phys. Res. A* **507**, 564–568 (2003).
18. M. A. Mackanos, J. A. Kozub, D. L. Hachey, K. M. Joos, D. L. Ellis, E. D. Jansen, "The effect of free-electron laser pulse structure on mid-infrared soft-tissue ablation: Biological effects," *Phys. Med. Biol.* **50**, 1885–1899 (2005).
19. Y. Nakajima, K. Iwatsuki, K. Ishii, S. Suzuki, T. Fujinaka, T. Yoshimine, K. Awazu, "Medical application of an infrared free-electron laser: Selective removal of cholesterol ester in carotid artery atheromatous plaques," *J. Neurosurg.* **104**, 426–428 (2006).
20. H. Hazama, Y. Takatani, K. Awazu, "Integrated ultraviolet and tunable mid-infrared laser source for analysis of proteins," *Proc. SPIE* **6455**, 645507 (2007).
21. M. A. Mackanos, D. Simanovskii, K. M. Joos, H. A. Schwettman, E. D. Jansen, "Mid infrared optical parametric oscillator (OPO) as a viable alternative to tissue ablation with the free electron laser (FEL)," *Lasers Surg. Med.* **39**, 230–236 (2007).
22. J. Kozub, B. Ivanov, A. Jayasinghe, R. Prasad, J. Shen, M. Klosner, D. Heller, M. Mendenhall, D. W. Piston, K. Joos, M. S. Hutson, "Raman-shifted alexandrite laser for soft tissue ablation in the 6- to 7-μm wavelength range," *Biomed. Opt. Express* **2**, 1275–1281 (2011).
23. G. S. Edwards, R. D. Pearlstein, M. L. Copeland, M. S. Hutson, K. Latone, A. Spiro, G. Pasmanik, "6450 nm wavelength tissue ablation using a nanosecond laser based on difference frequency mixing and stimulated Raman scattering," *Opt. Lett.* **32**, 1426–1428 (2007).
24. B. Choi, A. J. Welch, "Analysis of thermal relaxation during laser irradiation of tissue," *Lasers Surg. Med.* **29**, 351–359 (2001).
25. P. E. Dyer, "Laser ablation: Processes and applications," *Proc. SPIE* **3092**, 412 (1997).
26. J. M. Auerhammer, R. Walker, A. F. G. van der Meer, B. Jean, "Dynamic behavior of photoablation products of corneal tissue in the mid-IR: A study with FELIX," *Appl. Phys. B* **68**, 111–119 (1999).
27. K. Ishii, H. Tsukimoto, H. Hazama, K. Awazu, "Selective removal of cholesteryl ester in atherosclerotic plaque using nanosecond pulsed laser at 5.75 μm," *Proc. SPIE* **6854**, 685418 (2008).
28. T. Kita, K. Ishii, K. Yoshikawa, K. Yasuo, K. Yamamoto, K. Awazu, "Selective excavation of human carious dentin using the nanosecond pulsed laser in 5.8-μm wavelength range," *Proc. SPIE* **8566**, 85660B (2013).
29. T. Aellen, S. Blaser, M. Beck, D. Hofstetter, J. Faist, E. Gini, "Continuous-wave distributed-feedback quantum-cascade lasers on a Peltier cooler," *Appl. Phys. Lett.* **83**, 1929–1931 (2003).